JOURNAL OF MATERIALS SCIENCE 17 (1982) 3009–3016

Influence of heat treatment on the strength and fracture behaviour of Fe–12Cr–6Al ferritic stainless steel

SRINIVAS D. SASTRY, P. K. ROHATGI, K. P. ABRAHAM, Y. V. R. K. PRASAD
Department of Metallurgy, Indian Institute of Science, Bangalore, India

The changes in the tensile properties and fracture mode brought about by heat treatment of Fe–12Cr–6Al ferritic stainless steel have been studied. A favourable combination of high strength and good ductility is obtained by heating the material at 1370 K for 2 h followed by a water quench. The high-temperature treatment results in carbide dissolution as well as an increase in the grain size. The mechanism of strengthening has been evaluated from the apparent activation energy (28 kJ mol^{-1}) and is identified to be the unpinning of dislocations from the atmosphere of carbon atoms. As the heat-treatment temperature is increased, the fracture behaviour changes from ductile to brittle mode and this is related to the changes in grain size and friction stress.

1. Introduction

Ferritic stainless steels are usually Fe–Cr alloys containing 12–30% Cr and find important applications where high-temperature corrosion and oxidation resistance is a primary requirement [1]. These steels are widely used in applications such as automobile exhaust systems, jet engines, nuclear reactors and petroleum refineries [2]. The high-temperature oxidation resistance of Fe–Cr ferritic stainless steel is improved considerably by alloying it with aluminium [3]. It is also reported [3–5] that the addition of rare-earth elements gives oxidation resistance even under conditions of thermal cycling. However, the addition of Al to ferritic stainless steel is found to cause problems in mechanical processing as it drastically reduces the high-temperature ductility [6, 7]. The poor ductility of as-cast Fe–Cr–Al ferritic stainless steel is attributed to the presence of large alumina inclusions and coarse grain size [6].

The ferritic stainless steels are heat treated in a manner similar to austenitic stainless steels with a view to improving their ductility and corrosion resistance. But the high-temperature treatment of ferritic stainless steel is found [8–10] to cause embrittlement essentially brought about by a redistribution of interstitials in the ferrite matrix.

The aim of the present investigation is to study the effect of high-temperature treatment on the mechanical properties and fracture behaviour of Fe–12Cr–6Al ferritic stainless steel. The Fe–12Cr–6Al material was chosen for the present study because:

(i) a chromium content of 12% is considered optimum and is the minimum required for the stainless character [11]. Higher chromium contents will promote σ-phase precipitation [11] and restrict the permissible interstitial levels [12];

(ii) an aluminium content of 6% is again an optimum value for sufficient high-temperature oxidation resistance and for adequate ductility [7].

2. Experimental procedure

The preparation and mechanical processing of Fe–12Cr–6Al ferritic stainless steel were described in an earlier publication [13]. In brief, the material was prepared by melting Fe–13% Cr alloy in an induction furnace and deoxidizing the melt with Fe–Ti and misch metal. The Al addition was made by plunging an electrical-grade Al rod into the deoxidized molten bath. The melt was cast in permament moulds to obtain

0022–2461/82/103009–08$03.46/0

ingots of 75 mm diameter. The ingots were remelt refined using the electroslag refining process using a synthetic slag mixture containing CaF_2:CaO: Al_2O_3 in the proportions 60:20:20. The average chemical analysis (wt%) of the refined material was as follows: Cr – 12, Al – 6, Ti – 0.3, C – 0.12, P – 0.041, S – 0.01, N – 60 ppm, O – 30 ppm.

The refined ingots were hot-forged into slabs of 15 mm thick which were subsequently cold rolled into 1 mm thick sheets giving intermediate annealing treatments at 1220 K for 15 min whenever necessary. Sheet specimens with 15 mm gauge length, 3.5 mm width and 1 mm thick were milled from the rolled strips such that the rolling direction was parallel to their tensile axis. The tensile specimens were heated in the temperature range 1150–1500 K and for various holding times in the range 5 min to 4 h at each heat-treatment temperature. From the high temperature, one set of specimens was water-quenched and another set was air-cooled. A few specimens were also furnace-cooled. The room-temperature tensile properties were evaulated at a nominal strain rate of 10^{-3} sec^{-1} using a modified tensometer.

Specimens were prepared for optical microscopic examination following standard metallographic procedures. The etchant used consisted of H_2O_2 (10 vol%) and HF (15 vol%) in water. Microstructural details like inclusion content, grain size and carbide distribution were recorded. Specimens for transmission electron microscopy (TEM) were prepared first by chemically thinning the sheet to about 0.3 mm in a solution containing HNO_3 (30 vol%), HF (10 vol%) and HCl (15 vol%) in water and followed by electrochemical thinning. The electrochemical thinning was done in a solution containing 150 g CrO_3 and 750 ml acetic acid in 30 ml water at 25 V and 0.4 A. The fractured surfaces of tensile specimens were examined in a scanning electron microscope.

3. Results

3.1. Tensile properties at 300 K

The variation of yield strength with heat-treatment temperature for different holding times in water-quenched and air-cooled specimens is shown in Fig. 1. The yield strength of both water-quenched and air-cooled specimens increases with increasing

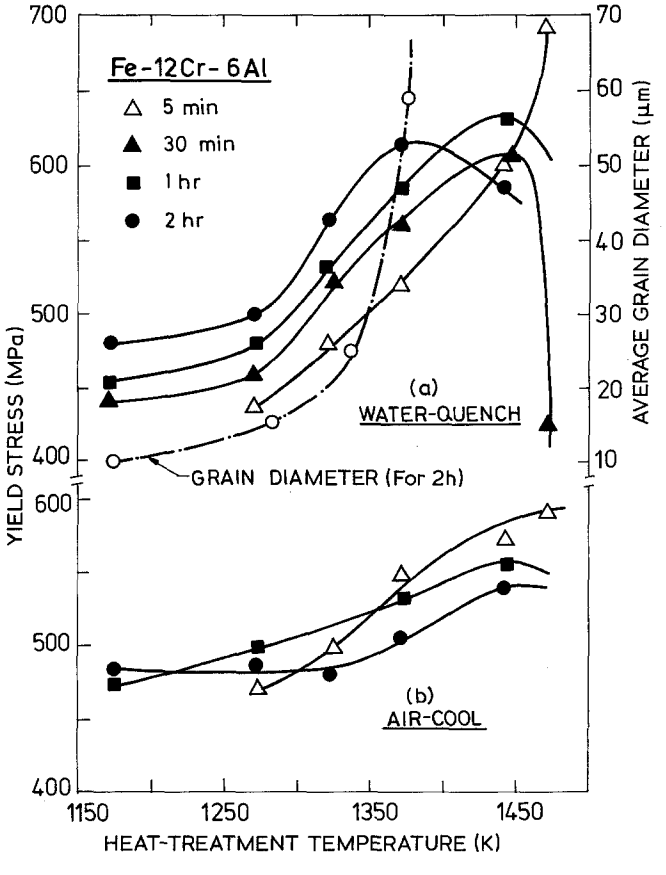

Figure 1 Variation of yield strength with heat-treatment temperature for different holding times: (a) water-quench; and (b) air-cool.

heat-treatment temperature from 1170 K onwards and reaches a peak. However, in the specimens heat treated for 5 min, the strength continues to increase with increase in heat-treatment temperature. The yield strength peaks are lower and shift to lower temperatures with increasing holding time in the water-quenched specimens. In the case of air-cooled specimens, the peaks and their shift with holding time are not well defined. Above 1370 K, the water-quenched specimens have higher yield strengths than the corresponding air-cooled specimens.

The tensile strength variation with heat-treatment parameters (Fig. 2a) is very similar to that described above. Ductility changes (elongation and reduction in area) in the water quenched specimens with heat-treatment temperature for different holding times are given in Fig. 2b. The ductility remains unchanged up to about 1370 K for all holding times and decreases rapidly for higher heat-treatment temperatures. The tensile strength and ductility variations in the air-cooled specimens are similar to those described above but are less prominent.

The rate of cooling from the heat-treatment temperature has a significant effect on the strength but not on the ductility as shown in Table I, for specimens heat treated at 1370 K for 2 h. Lower rates of cooling give lower strength values.

The variation of yield strength with holding time for different heat-treatment temperatures in the range 1170–1470 K is shown in Fig. 3. The yield strength reaches a peak value for all temperatures, the time taken to reach the peak being smaller at higher temperatures.

3.2. Microstructural features

The optical micrographs recorded on specimens heat treated at 1270 K for peak strength have shown carbide precipitation both at grain boundaries and in the interior of the grains. The higher the heat-treatment temperature, the more is the carbide dissolution and the greater the grain size. Increasing the holding time has helped in carbide dissolution and in increasing the grain size.

The volume fraction of carbides is estimated from the microstructure and is given in Fig. 4 as

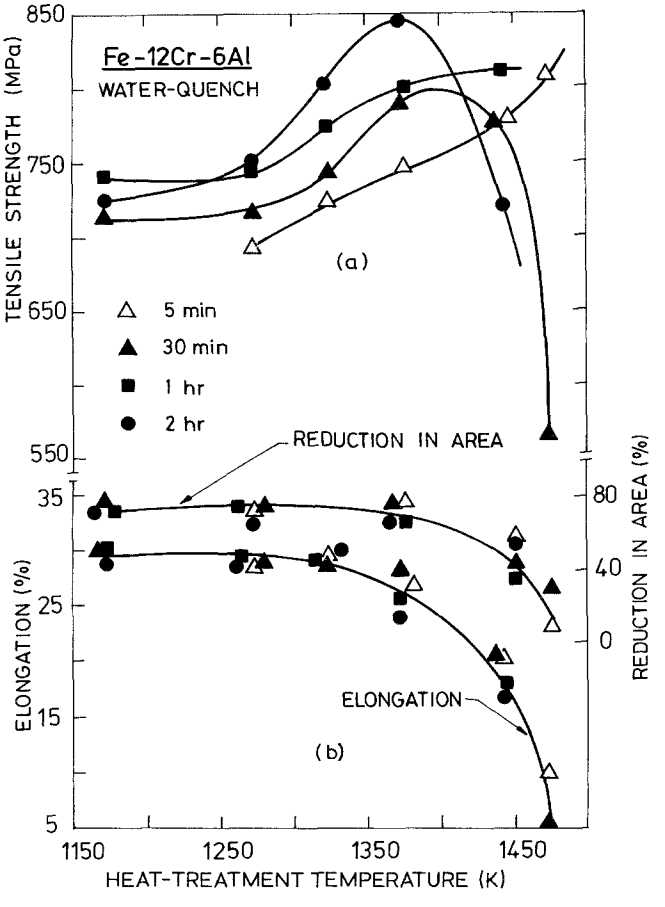

Figure 2 Variation of tensile strength and ductility with heat-treatment for different holding times.

TABLE I Effect of cooling rate on the tensile properties in 1370 K–2 h treated specimens

Cooling method	Yield strength (MPa)	Tensile strength (MPa)	Elongation (%)	Reduction in area (%)
Water-quenched	613	850	25	65
Air-cooled	503	701	20	73
Furnace-cooled	447	663	24	69

a function of heat-treatment variables: the holding time at 1370 K (Fig. 4a) and at time-to-peak at different heat-treatment temperatures (Fig. 4b). The grain-size variations with heat-treatment temperature and holding time are represented in Fig. 1 and Fig. 3, respectively. The grain growth occurs predominantly beyond 1370 K and about 2 h holding time at this temperature. At temperatures higher than 1370 K, grain growth readily occurs even in much shorter holding times than 2 h.

3.3. Fractography

The SEM fractographs obtained on the heat-treated specimens fractured at room temperature are shown in Fig. 5. The figure includes the SEM picture on specimens heat treated at 1170 K (0.5 h), 1370 K (2 h) and 1470 K (0.5 h) followed by a water-quench. Fig. 5 reveals that the 1170 K specimen fails by a ductile mode (Fig. 5a) and the 1470 K specimen undergoes a brittle failure (Fig. 5c). A mixed mode of failure is observed in the 1370 K specimen (Fig. 5b).

The effect of cooling rate on the mode of failure in the 1370 K–2 h treated specimen tested at room temperature is depicted in Fig. 6. Comparing this with Fig. 5b, it is seen that the slower rate of cooling (air-cooling or furnace-cooling) prevents the occurrence of cleavage.

4. Discussion

4.1. Strengthening mechanism in heat-treated Fe–12Cr–6Al

Unlike austenitic stainless steels, the commercial purity Fe–12Cr–6Al ferritic stainless steel is strengthened by heat treatment involving high-temperature exposure followed by water-quench. As shown in Figs. 1–3, the extent of strengthening depends on the heat-treatment variables: the temperature and the holding time. The observed strengthening due to heat treatment might have been caused by any one of the following mechanisms:

(i) solid-solution strengthening by Al [14];

(ii) reprecipitation of carbides on dislocations during cooling as suggested by Demo [10];

(iii) formation of austenite in the grain-boundary regions due to carbon segregation and transformation of martensite on quenching [9];

(iv) formation of a high-temperature phase similar to "chi" phase observed in the Fe–Cr–Mo system [15];

(v) grain boundary strengthening;

(vi) strengthening caused by quenched-in dislocations;

(vii) dissolution of carbides or nitrides at high temperature making free carbon or nitrogen available in the bcc matrix for strengthening by Cottrell locking.

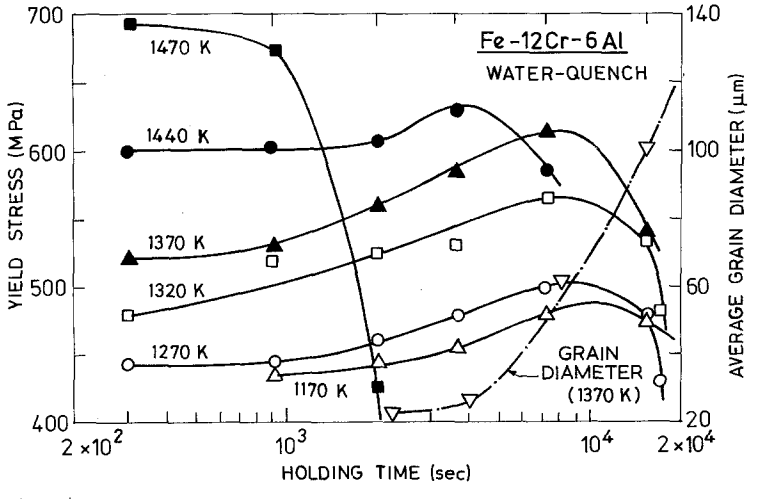

Figure 3 Variation of yield strength with holding time for different heat-treatment temperatures.

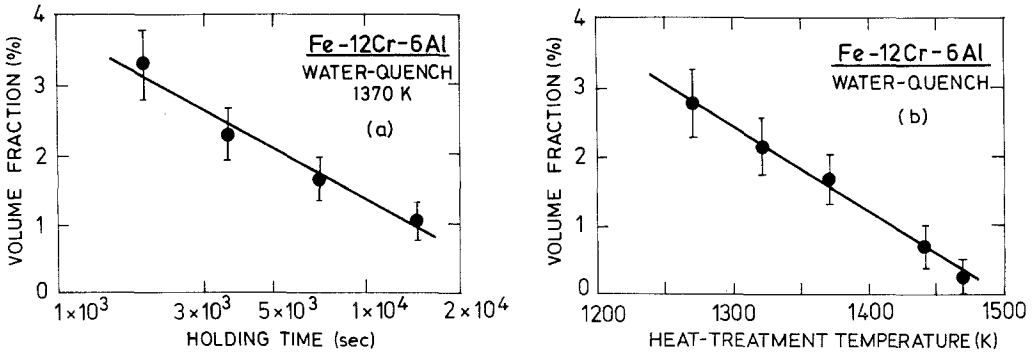

Figure 4 Variation of the amount of carbides in specimens (a) heat treated at 1370 K for different holding times, and (b) heat treated for peak strength at different temperatures.

In view of the large size difference between Fe and Al atoms (≈ 12%), the addition of Al to Fe causes substantial solid-solution strengthening. However, from the Fe–Al phase diagram [16] it is seen that the solid solubility of Al in Fe at room temperature is about 10 wt% and increases to 20 wt% at 1470 K. As the alloy with 6% Al is single-phase in the temperature range of heat treatment, no additional strengthening due to Al is achieved by heat treatment. The transmission electron micrographs did not reveal any preferential carbide precipitation on dislocations. The micrograph recorded on the thin foil of a 1370 K–2 h water-quenched specimen is given in Fig. 7. The observed strengthening cannot, therefore, be accounted for on the basis of the reprecipitation model.

In the Fe–Cr–Mo system, the formation of "chi"-phase (bcc) at high temperatures is reported [15]. In addition to a high-temperature phase, it is possible that an intermetallic Fe_3Al may form in the Fe–Cr–Al system. TEM studies on the heat-treated specimens did not reveal the presence of any second phase other than chromium carbide ($M_{23}C_6$). Thus, there is also no evidence in support of a high-temperature phase being responsible for the strengthening.

The metallographic examination has revealed that the grain size increases with increasing heat-treatment temperature as well as the holding time. It is well known that the grain-size dependence of strength follows the Hall–Petch relation [17]

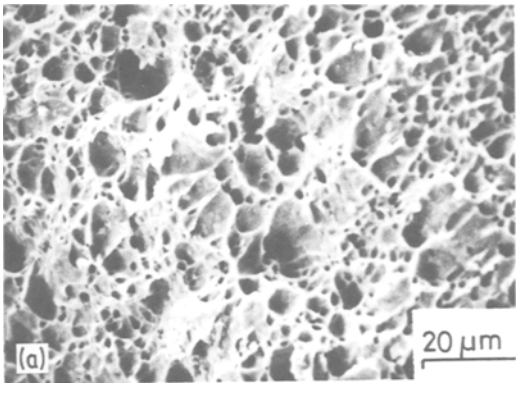

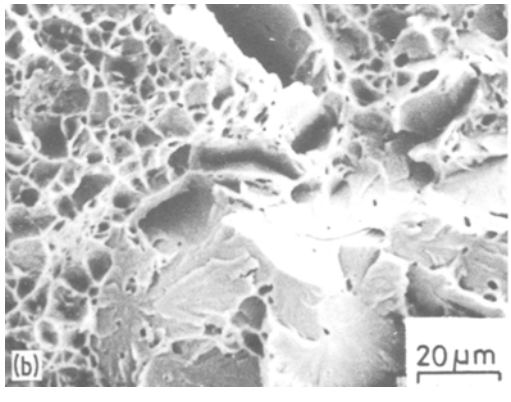

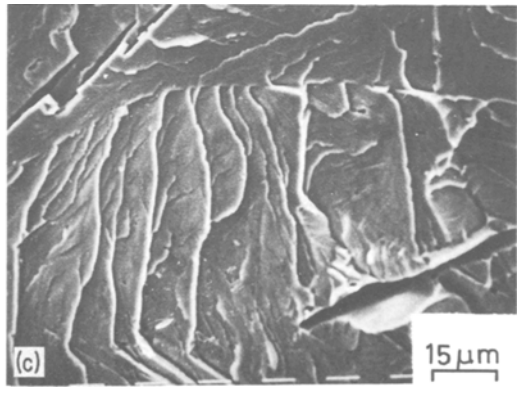

Figure 5 SEM fractographs of heat-treated specimens (a) 1170 K–0.5 h, (b) 1370 K–2 h and (c) 1470 K–0.5 h followed by water-quench.

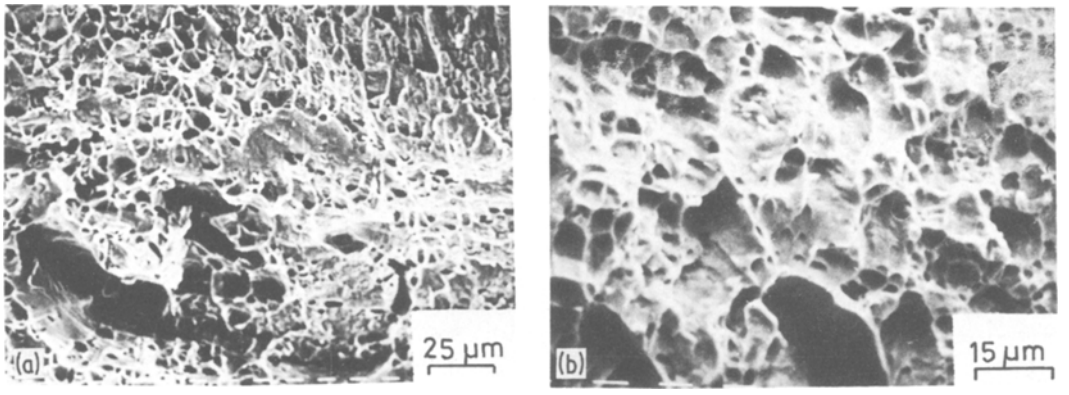

Figure 6 SEM fractographs of specimens heat treated at 1370 K– 2 h (a) air-cooled, and (b) furnace-cooled.

according to which the room-temperature yield strength increases linearly with $d^{-1/2}$ where d is the average grain diameter. A comparison of the grain-size data and the yield strength data given in Figs. 1 and 3 shows that the increase in the strength up to the peak cannot be explained on the basis of grain-size variations. However, the drop in the strength beyond the peak is clearly due to the occurrence of grain growth. Thus the strengthening cannot be related to grain-size variations caused by the heat treatment.

The dissolution of carbides at high temperatures makes available free carbon in the ferrite matrix which on quenching is retained in solution. The higher the heat-treatment temperature or the holding time, the larger is the extent of carbide dissolution and therefore the higher is the carbon in solution. This gives considerable strengthening of the ferrite matrix by Cottrell atmosphere formation around dislocations [18]. A model based on coherent state theory similar to that described above was postulated by Thielsch [8] for the high-temperature embrittlement in ferritic stainless steels. Solid-solution strengthening by C and N during the heat treatment of Fe–Cr alloys was also reported by Hitoshi and Yoshinori [19]. The contribution to the increase in the yield stress from differences in the quenched-in dislocation density will be small in comparison with the interstitial effect.

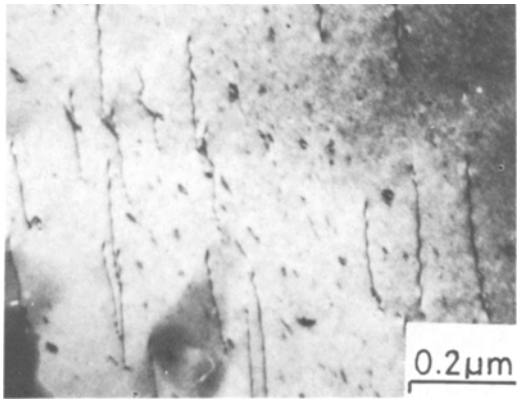

Figure 7 Transmission electron micrograph of 1370 K– 2 h water-quenched specimen.

The amount of interstitials in solution is governed by the dissolution of carbides or nitrides at the heat-treatment temperature (T) through an Arrhenius type of equation:

$$c = \text{Constant}.\exp(-Q/RT) \qquad (1)$$

where c is the concentration of interstitials and Q is the activation energy for diffusion. Taking the yield stress to be proportional to the interstitial content, it is possible to estimate the apparent activation energy by plotting log(yield stress) as a function of $(1/T)$. In Fig. 8, the peak yield-strength values are plotted as a function of heat-treatment temperature. The effect of increase in grain size on yield stress will be negligible at holding times lower than the time-to-peak. This is seen by plotting the yield stress at a holding time of 1 h as a function of $(1/T)$ which is also shown in Fig. 8. The slopes of the peak yield-stress line matches well with that obtained at 1 h holding time. The apparent activation energy estimated from Fig. 8 is 28 kJ mol^{-1}.

The activation energy for the strengthening by Cottrell atmosphere formation of C atoms is that required for the unpinning of dislocations. The binding energy between dislocations and carbon atoms [14] is 48 kJ mol^{-1}, while the activation energy for the unpinning, being stress-

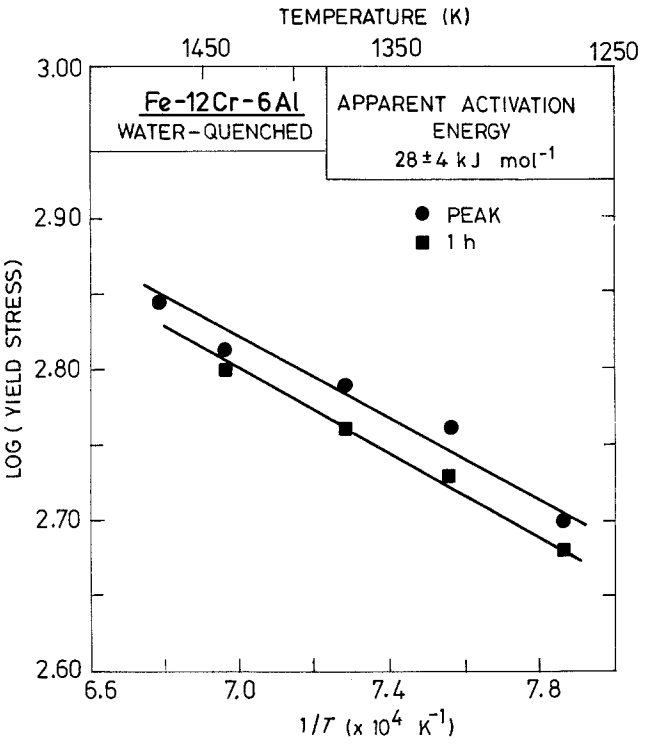

Figure 8 Arrhenius plot showing the variation of yield strength with inverse of heat-treatment temperature.

aided, is lower [20] (31 kJ mol^{-1}). The apparent activation energy presently estimated for the strengthening (28 kJ mol^{-1}) matches well with that for the unpinning mechanism. The estimate for the apparent activation energy obtained from the hardness data [21] (33 kJ mol^{-1}) on Fe–12Cr–6Al material also agrees with the above.

The influence of cooling rate on the strengthening is in terms of controlling the amount of reprecipitation of carbides during cooling. Higher cooling rates reduce the reprecipitation and retain more carbon in solution causing an increase in strength (Table I).

The binding energy between dislocations and Al atoms is also of the order of 48 kJ mol^{-1} on the basis of the atomic size difference [14], and the activation energy for unpinning is likely to be of the same order as that for unpinning of C atoms. However, the strengthening due to Al atoms does not respond to heat treatment and hence is not responsible for the observed strengthening brought about by heat treatment.

4.2. Fracture mechanism in heat-treated Fe–12Cr–6Al

The effect of grain size on the yield stress, σ_y, and the brittle fracture sttress, σ_F, is related by a Hall–Petch type of relation [17, 22, 23]:

$$\sigma_y = \sigma_{0y} + k_y d^{-1/2} \quad (2)$$

$$\sigma_F = \sigma_{0F} + k_F d^{-1/2} \quad (3)$$

where σ_{0y} and k_y are the intercept and slope, respectively, of the plot of σ_y against $d^{-1/2}$ while σ_{0F} and k_F are the intercept and slope of the plot of σ_F against $d^{-1/2}$. σ_F is generally temperature-independent whereas σ_y increases with decrease in temperature. At a given testing temperature, there is a critical grain size defined at $\sigma_y = \sigma_F$ above which brittle fracture is favoured. In addition, an increase in the friction stress, σ_{0y}, lowers the critical grain size [23]. Thus, brittle fracture is promoted by an increase in grain size as well as an increase in the friction stress.

The large grain size (102 μm) and the high friction stress caused by the dissolved carbon in the 1470 K–water-quenched specimen, induces brittle failure at room temperature (Fig. 5c). In contrast, the 1170 K–water-quenched specimen which has a finer grain size ($\approx$ 10 μm) and lower friction stress (carbon being in the combined form as carbide) undergoes a ductile rupture (dimples) (Fig. 5a). The specimen water-quenched from 1370 K has a grain size (50–70 μm) and a friction stress that is about the critical value required for causing a transition from one to another mode and hence shows a mixed mode of failure (Fig. 5b). It

is, however, difficult to separate the grain size and the friction stress effects on the yield and fracture in Fe–12Cr–6Al ferritic stainless steel as any heat treatment given to change the friction stress also varies the grain size.

The change in the mode of failure from a mixed one (Fig. 5b) to a ductile one (Fig. 6a, b) with decrease in cooling rate is attributed to a lowering of friction stress caused by the reprecipitation of carbides.

5. Conclusions

(i) The tensile properties of Fe–12Cr–6Al ferritic stainless steel depend on the heat-treatment temperature, holding time and the rate of cooling.

(ii) The best combination of strength and ductility is obtained by heating the material for 2 h at 1370 K followed by a water-quench.

(iii) The apparent activation energy estimated from the dependence of yield strength on heat-treatment temperature is $28\,kJ\,mol^{-1}$ which suggests that the strengthening mechanism is the unpinning of dislocations from the atmosphere of carbon atoms. The dissolution of carbides at high temperature followed by water-quench retains carbon in solution thereby forming an atmosphere.

(iv) The mode of tensile failure at room temperature is a function of heat-treatment variables. Specimens heat treated to give a microstructure with large grain size ($102\,\mu m$) and high stress show a brittle failure while fine-grained microstructure with carbides give ductile rupture (dimples). A mixed mode of failure occurs for critical grain size ($50–70\,\mu m$) and friction stress.

Acknowledgements

The authors are grateful to the authorities of the National Aeronautical Laboratory, Bangalore and Reactor Research Centre, Kalpakkam, for extending their Instron and Electron Microscope facilities, respectively.

References

1. A. ROY, F. A. HAGEN and J. M. CORWIN, SAE Paper 740093 (1974).
2. P. M. GILES, H. ABRAMS and A. R. MARDER, US Pat. 3 873 306 (1975).
3. I. KVERNES, M. OUVEIRA and P. KOFSTAD, *Corrosion Sci.* **17** (1977) 237.
4. F. A. GOLIGHTLY, F. H. STOTT and G. C. WOOD, *Oxid. Met.* **10** (1976) 163.
5. S. KUNIO, *Japan Kokai,* 76 38 217 (Cl.C22c 38/18) (1976).
6. R. CHOUBEY, B. N. DAS and B. R. NIJHAWAN, "Proceedings of Symposium on Metallurgical Substitutes for Ferrous and Non-ferrous Alloys" (National Metallurgical Laboratory, Jamshedpur, India, 1966) p. 133.
7. A. ROY and J. M. CORWIN, *Met. Prog.* **95** (1969) 70.
8. H. THIELSCH, *Welding J.* **34** (1959) 225.
9. T. A. PRUGER, *Steel Horizon* **13** (1951) 10.
10. J. J. DEMO, *Corrosion* **27** (1971) 531.
11. G. J. FISHER and R. J. MACIAG, "Handbook of Stainless Steels" (McGraw-Hill, New York, 1977) p. 1.
12. I. A. FROMSON, *Met. Trans.* **5** (1974) 2257.
13. S. D. SASTRY, P. K. ROHATGI, K. P. ABRAHAM and Y. V. R. K. PRASAD, *Met. Tech.* **7** (1980) 393.
14. J. FRIEDEL, "Dislocations" (Pergamon Press, London, 1964) p. 379.
15. J. G. McMULLEN, S. F. REITER and D. G. EBELING, *Trans. ASM,* **46** (1954) 799.
16. "Metals Hand Book", 8th edn, Vol. 8 (ASM, Metals Park, Ohio, 1973) p. 260.
17. R. W. ARMSTRONG, I. CODD, R. M. DOUTHWAITE and N. J. PETCH, *Phil. Mag.* **7** (1962) 45.
18. A. H. COTTRELL, "Dislocations and Plastic Flow in Crystals" (Oxford University Press, New York, London, 1953).
19. I. HITOSHI and F. YOSHINORI, *Nippon Kinzoku Gakkaishi* **39** (1975) 311.
20. F. H. WOHLBIER (ed), "Diffusion and Defect Data Book", Vol. 14 (Trans Tech Publications, Rockport, Massachussets, 1977) p. 42.
21. S. D. SASTRY, P. K. ROHATGI, K. P. ABRAHAM and Y. V. R. K. PRASAD, *Scripta Metal.* **13** (1979) 819.
22. J. R. LOW, "Relation of Properties to Microstructure" (ASM, Metals Park, Ohio, 1954).
23. R. W. ARMSTRONG, *Met. Trans.* **1** (1970) 1169.

Received 6 January
and accepted 22 March 1982